Journal of Inflammation Research

Dovepress
Taylor & Francis Group

Open Access Full Text Article

ORIGINAL RESEARCH

# Mechanistic Perspectives on Radiation-Induced Skin Injury and the Protective Effects of Berberine

Biao Huang[1,*], Gong Chen[2,*], Tao Yan[1,*], Xiaolan Ou[1], Long Yang[2], Tinghao He[2], Fenghao Geng[3], Zehua Zhou[1], Guozhong Lyu[4], Shuyu Zhang[3], Daojiang Yu[1,4]

[1]Department of Plastic and Burn Surgery, The Second Affiliated Hospital of Chengdu Medical College, Nuclear Industry 416 Hospital, Chengdu, 610051, People's Republic of China; [2]Department of Medicine, Chengdu Medical College, Chengdu, 610051, People's Republic of China; [3]Laboratory of Radiation Medicine, West China School of Basic Medical Sciences and Forensic Medicine, Sichuan University, Chengdu, 610041, People's Republic of China; [4]Department of Burn and Plastic Surgery, Affiliated Hospital of Jiangnan University, Wuxi, 214122, People's Republic of China

*These authors contributed equally to this work

Correspondence: Shuyu Zhang, Laboratory of Radiation Medicine, West China School of Basic Medical Sciences and Forensic Medicine, Sichuan University, Chengdu, 610041, People's Republic of China, Email zhangshuyu@scu.edu.cn; Daojiang Yu, Department of Plastic and Burn Surgery, The Second Affiliated Hospital of Chengdu Medical College, Nuclear Industry 416 Hospital, Chengdu, 610051, People's Republic of China, Email ydj51087@163.com



**Background:** Radiation-induced skin injury (RISI) is a common complication of radiotherapy, affecting up to 95% of cancer patients. It manifests as acute erythema and ulceration or chronic fibrosis and telangiectasia, severely compromising patients' quality of life. The pathogenesis of RISI involves oxidative stress, inflammation, DNA damage, and cellular senescence. However, current treatments are largely supportive and fail to address underlying mechanisms. Berberine (BBR), a natural isoquinoline alkaloid, exhibits anti-inflammatory, antioxidant, and wound-healing properties, making it a promising candidate for managing RISI.

**Methods:** Single-cell RNA sequencing and proteomic analyses were employed to characterize the molecular and cellular changes in patient, rats and cells exposed to ionizing radiation. Differentially expressed genes (DEGs) and proteins were identified, and functional enrichment analyses were performed. Key senescence markers were validated using molecular docking and in vitro assays. The therapeutic effect of BBR was validated in skin cells and in mouse models of radiation-induced skin injury, focusing on wound healing and systemic health.

**Results:** Transcriptomic analysis identified 217 DEGs in RISI, highlighting pathways such as TNF, p53, and NF-kappa B signaling. Key senescence markers, including CDKN1A, IGFBP7, and CTSL, were overexpressed, correlating with impaired wound healing. Proteomic analysis revealed that BBR modulated 684 proteins, enhancing keratinocyte migration and reducing oxidative damage. BBR treatment promoted the proliferation and migration of skin cells, alleviated radiation-induced cellular senescence, and downregulated inflammatory pathways including p53, ROS, and JAK-STAT. BBR-treated mice exhibited significantly reduced skin injury scores, improved body weight retention, and enhanced wound healing.

**Conclusion:** Radiation injury leads to persistent senescence, inflammation, and impaired wound healing in skin tissues. CDKN1A, IGFBP7, and CTSL are core senescence markers in RISI. By downregulating the expression of senescence markers and suppressing inflammatory pathways (including p53, ROS, and JAK-STAT), BBR accelerates radiation-induced wound healing, offering a novel therapeutic strategy for managing RISI.

**Keywords:** radiation-induced skin injury, berberine, cellular senescence, proteomics, single-cell RNA sequencing, wound healing

## Introduction

Radiation-induced skin injury (RISI) is a prevalent complication arising from radiotherapy, affecting up to 95% of patients undergoing treatment for malignant tumors.[1] These injuries can manifest acutely as erythema, dry or moist desquamation, and, in severe cases, ulceration.[2] Chronic effects may include fibrosis, telangiectasia, and persistent ulcerations, all of which significantly diminish patients' quality of life and can impede the continuation of essential cancer therapies.[3]



Received: 24 March 2025
Accepted: 11 July 2025
Published: 12 August 2025

The pathogenesis of RISI is multifaceted, involving oxidative stress, inflammatory responses, DNA damage, and cellular senescence.[4,5] Ionizing radiation generates reactive oxygen species (ROS), leading to direct cellular damage and the activation of pro-inflammatory cytokines and chemokines.[6,7] This cascade results in endothelial dysfunction, fibroblast activation, and subsequent tissue remodeling, culminating in the clinical manifestations of skin injury.[8]

Despite the high incidence of RISI, there is no universally accepted standard treatment. Current management strategies are primarily supportive, focusing on symptom relief and prevention of secondary infections.[9] Topical corticosteroids, emollients, and dressings are commonly employed, yet their efficacy varies, and they do not address the underlying pathophysiological mechanisms.[10] Merely employing local wound care is frequently insufficient in arresting the advancement of radiation-induced damage, given the enduring ROS-mediated injury, prolonged inflammatory reactions, and cellular senescence observed in irradiated tissues.[6,11] Hence, the critical imperative lies in the development of therapeutic agents that address the fundamental mechanisms of radiation injury to mitigate clinical manifestations and enhance tissue regeneration in patients.

Berberine (BBR), a natural isoquinoline alkaloid, has garnered attention for its diverse pharmacological properties, including anti-inflammatory, antioxidant, and antimicrobial effects.[12] Plants belonging to the Berberis genus are the most widely distributed natural source of berberine.[13] Berberine is the primary active component of the medicinal plant Coptis chinensis and is widely used in the treatment of diabetes and cardiovascular diseases.[14,15] Recent studies have demonstrated BBR's potential in mitigating radiation-induced injuries in various tissues. For instance, BBR has been shown to reduce the incidence and severity of radiation-induced lung injury in patients with non-small cell lung cancer.[16] Li et al found that berberine treatment can delay mortality and alleviate intestinal injury in mice undergoing total abdominal irradiation.[17] Additionally, BBR has been reported to alleviate delayed healing of skin wounds by activating NRF2, a key regulator of cellular antioxidant responses.[18] However, there have been few studies on the role and mechanism of BBR in radiation-induced skin injury. In acute toxicity studies in mice, the LD50 of pure berberine was determined to be 329 mg/kg, and it is considered safe at normal oral dosage levels.[19]

Given the complex pathophysiology of RISI and the limitations of current treatments, exploring novel therapeutic agents like BBR is imperative. This study establishes animal and cellular models and employs single-cell transcriptomic analysis to reveal cellular and molecular-level changes in radiation-induced skin injury. This study identified core senescence-related targets in RISI and revealed that BBR may ameliorate radiation damage by modulating these senescence targets and inflammatory pathways (p53, ROS, and JAK-STAT signaling), providing a potential therapeutic strategy to promote skin repair and improve patient outcomes.

# Materials and Methods

## Sample Source and Single Cell Sequencing

Irradiated skin samples were obtained from a victim of an iridium radiation accident, as previously reported.[20] The samples were taken from the right hand, which had been exposed to an iridium-192 (192Ir) metal chain with an activity of 966.4 GBq (26.1 Ci). Normal skin tissue was sourced from the patient's navel for comparison. Ethical and legal approval was obtained prior to the commencement of the study. This study was approved by the Medical Ethics Committee of the Second Affiliated Hospital of Chengdu Medical College, Nuclear Industry 416 Hospital. All participants provided written informed consent. All experiments were performed following Medical Ethics Committee of the second affiliated hospital of Chengdu medical college and national guidelines and regulations. The present study was conducted in accordance with the Declaration of Helsinki.

Based on the 10xGenomics platform, microfluidic technology is used to wrap beads and cells with CellBarcode in droplets, and the droplets containing cells are collected.[21] The cells are then lysed in the droplets, allowing the mRNA in the cells to combine with the CellBarcode on the bead to form SingleCellGEMs. Then a reverse transcription reaction is performed in the droplets to construct a cDNA library, and the sample source of the target sequence is distinguished through the sample index on the library sequence. Single-cell sequencing data has been uploaded to GEO public database and can be accessed using the provided identifier GSE193564 and GSE193807.[22]

## Bioinformatic Analysis

The Cell Ranger software pipeline (version 5.0.0) provided by 10×Genomics was used to demultiplex cellular barcodes, map reads to the genome and transcriptome using the STAR aligner, and down-sample reads as required to generate normalized aggregate data across samples, producing a matrix of gene counts versus cells.

Principal component analysis (PCA) was performed to reduce the dimensionality with RunPCA function in Seurat.[23] Graph-based clustering was performed to cluster cells according to their gene expression profile using the FindClusters function in Seurat. Cells were visualized using a 2-dimensional t-distributed stochastic neighbor embedding (t-SNE) algorithm with the RunTSNE function in Seurat. We used the R package SingleR,[24] a novel computational method for unbiased cell type recognition of scRNA-seq, with the reference transcriptomic datasets "Human Primary Cell Atlas" to infer the cell of origin of each of the single cells independently and identify cell types.[25]

Differentially expressed genes (DEGs) between RISI and normal skin were identified using the FindMarkers function (test.use = MAST) in Seurat. Adjusted p-value < 0.05 and FC > 1.5 or FC < 0.67 were set as the thresholds for significant differential expression.

## Senescence-Related Gene List and Normal Wound Data

Senescence-related genes could be found in the GeneCards (https://www.genecards.org/) databases by searching the keyword "Cell senescence", and the retrieved targets were combined.[26] We have provided the list of senescence-related genes in Supplementary File 1. Additionally, transcriptomic data for normal wound healing on day 1 and day 7, as well as chronic ulcer wounds, can also be accessed from the GEO database under the accession number GSE174661.[27] Using the transcriptomic data from acute wound mentioned above, we investigated the correlation of the core genes with normal wound healing.

## GO and Pathway Enrichment Analysis

GO function and KEGG pathway-enrichment analyses were performed using cluster Profiler R package for the DEGs of RISI, with p set at <0.01 and FDR set at <0.05. Meanwhile, we performed pathway enrichment analysis of the core genes using the Reactome database.[28]

## Protein–Protein Interaction Network Construction

The intersecting target genes were uploaded to the String database (http://string-db.org/), the organisms were limited to "Homo sapiens" and the medium confidence was set to be less than 0.4; then, the relationship between the target proteins was obtained. Afterwards, the interaction network between core genes and transcription factors was visualized using Cytoscape 3.9.0 software.

## Molecular Docking

The 3D structure of the core target of BBR that acted on RISI was searched from the PDB database (https://www.rcsb.org/).[29] We downloaded the crystal structures of core targets from the PDB library: CDKN1A (1AXC), IGFBP7 (8IVD) and CTSL (8GX2). For docking analysis, all protein and molecular files were converted into PDBQT format with all water molecules excluded and polar hydrogen atoms were added. The grid box was centered to cover the domain of each protein and to accommodate free molecular movement. The grid box was set to 30 Å × 30 Å × 30 Å, and grid point distance was 0.05nm. Molecular docking studies were performed by Autodock Vina 1.2.2.[30] Finally, the PyMOL software was used in drawing.

## Cell Culture, Treatment and Protein Extraction

Human umbilical vein endothelial cells (Huvecs) were procured from the Chinese Academy of Sciences (Shanghai, China). Huvecs were cultured, as previously described.[31] Cells were seeded in flat-bottom 6-well plates and cultured until they reached 80% to 90% confluence, and medium was replaced with fresh medium. After further cultivation for 24 hours, cells were stimulated with irradiation (5Gy; Sigma-Aldrich) and/or treated with different doses of BBR (from 5uM to 20uM) at 37.0°C in 5% CO2 and incubated for another 16 hours, as previously reported.[32] The berberine used in this study was

purchased from Selleck Chemicals (https://www.selleck.cn/products/berberine.html) with a purity of 99.02%. Next, the cells were harvested and subjected to proliferation and apoptosis experiment. To induce senescent cells, the Huvecs were exposed to radiation with a total dose of 5 Gy. Then, the irradiated Huvecs were cultured normally for 7 days and the senescent phenotypes and ROS of the endothelial cells were identified by SA-β-gal staining and immunofluorescence staining.

For protein extraction, the sample was grinded with liquid nitrogen into cell powder and then transferred to a 5-mL centrifuge tube. After that, four volumes of lysis buffer (8 M urea, 1% protease inhibitor cocktail) were added to the cell powder, followed by sonication three minutes on ice using a high intensity ultrasonic processor (Scientz). (Note: For PTM experiments, inhibitors were also added to the lysis buffer, eg 3 μM TSA and 50 mM NAM for acetylation, 1% phosphatase inhibitor for phosphorylation). The remaining debris was removed by centrifugation at 12,000 g at 4 °C for 10 min. Finally, the supernatant was collected and the protein concentration was determined with BCA kit according to the manufacturer's instructions. The procedure involves using bovine serum albumin (BSA) as a standard, mixing BCA reagents A and B (25 μL sample + 200 μL working solution), and incubating at 37°C for 30 minutes. The absorbance of the reaction product is then measured at a wavelength of 562 nm using a UV-Vis spectrophotometer.

## Establishment and Treatment of Radiation Animal Models

The animal studies were in accordance with the animal care and use committee of the Chengdu medical college. Ethical and legal approval was obtained prior to the commencement of the study (ethical approval number DWSB-2024-026). This study was approved by the Medical Ethics Committee of the second affiliated hospital of Chengdu Medical College (Nuclear Industry 416 Hospital).

Male mice (C57BL/6, 6–8 weeks) purchased from the laboratory animal center of Chengdu medical college were used to establish radiation ulcer models. A power analysis was conducted before the experiment to determine the sample size. All animals (n=18) were randomly divided into three groups: a radiation injury group (n=6), a radiation injury treated with BBR group (n=6) and a control group (n=6). Mice were kept in cages (23°C) on a 12-hour light/dark cycle with ad libitum access to food and water. All applicable international, national, and institutional guidelines for the care and use of animals were followed. Environmental adaptation 3 days before radiation experiment. The mice in the BBR treatment group were intragastrically administered BBR once daily at a dose of 50 mg/kg for 3 days prior to irradiation. For radiation injury, mice limb skin radiation ulcer models were established as previously described.[33] In brief, 1% pentobarbital sodium was used for anesthesia, and mice' posterior limbs were irradiated with 10 Gy of 160 kVp X-ray (RADSOURCERS 2000 X-ray machine, USA) at a dose rate of 1.20 Gy/min for 8–9 minutes, with a total dose of 20 Gy (precision X-ray; fractionated radiation). Other body parts were shielded with lead plates. The skin injury recovery process in IR and BBR treatment mice were evaluated for 34 d, and pictures were taken of the wound site. Weigh the mice every 3 days. The skin injury score scale from 1 (no damage) to 5 (severe damage), as previously described.[34] Two experienced observers scored the skin damage under blinded conditions.

## Statistical Analysis

The number of biological replicates used in each experiment is indicated in the respective method sections and figure legends. Comparisons between groups were performed using paired or unpaired Student's *t*-test, one-way analysis of variance (ANOVA), or two-way ANOVA. Differential expression, GO and KEGG functional annotation, and proteomics analysis were all performed and visualized using R software. In all tests, a p-value $< 0.05$ or a false discovery rate (FDR) $< 0.05$ was considered the threshold for statistical significance. Statistical analysis was performed using GraphPad Prism software version 9.

# Results

## Transcriptomic Changes in Irradiated Patient Skin

Through differential analysis between irradiated and non-irradiated areas (Figure 1A), we identified 217 differentially expressed genes, comprising 116 upregulated and 101 downregulated genes (Figure 1C). A heat map, based on fold changes, illustrates the gene expression differences induced by radiation injury (Figure 1B). The most significantly

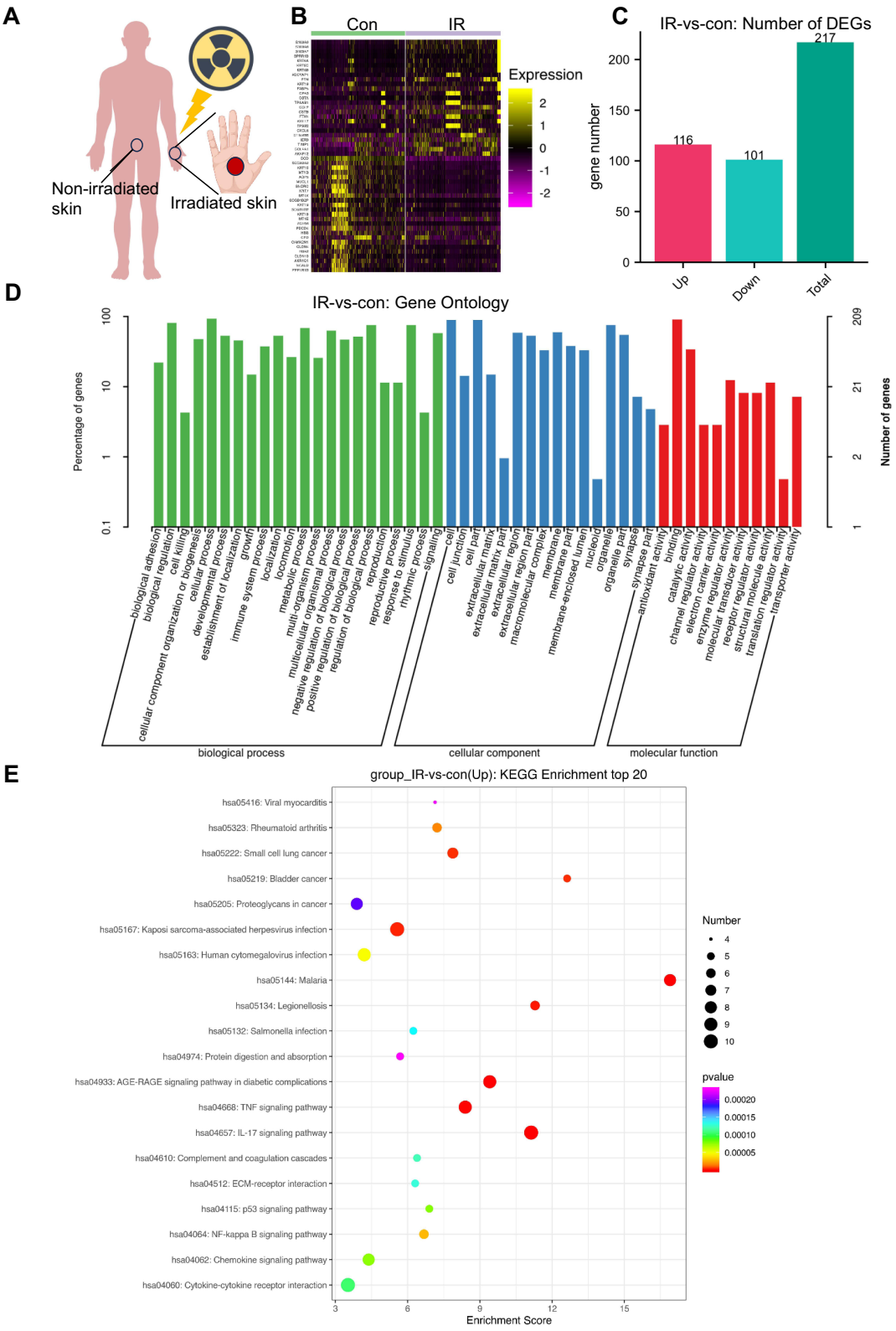


**Figure 1** Collection of irradiated Tissues and Their Transcriptomic changes. (**A**) Schematic diagram of the tissue extraction workflow. (**B**) Heatmap of differentially expressed genes. (**C**) Statistical analysis of differentially expressed genes. (**D** and **E**) GO and KEGG pathway enrichment analysis of DEGs.
**Abbreviations**: DEGs, differentially expressed genes; GO, gene ontology; KEGG, Kyoto Encyclopedia of Genes and Genomes.


https://doi.org/10.2147/JIR.S523616

upregulated genes after radiation injury include S100A8 (log2Fold Change=3.79, adjust<0.05) and S100A9 (log2Fold Change=4.27, adjust<0.05), which are associated with inflammation and ulcer.[35,36] Conversely, the most significantly downregulated genes include DCD, KRT15, and AQP5, which are implicated in skin barrier function.

## GO and KEGG Analysis

Function annotation has been carried out among 217 differentially expressed genes (P<0.01; FDR<0.01). BP category suggested that biological adhesion, cell killing, cellular process, immune system process and response to stimulus were important process of differentially expressed genes. In addition, MF results indicated that these genes were mostly involved in antioxidant activity, binding and catalytic activity. While, the main CC category of these genes included cell junction, cell part, extracellular matrix part items (Figure 1D).

In KEGG results, we found that radiation injury upregulated several tumor-associated pathways, as well as multiple inflammation and DNA damage-related pathways, including TNF, P53, NF-kappa B, and AGE-RAGE signaling pathways (Figure 1E).

## Radiation Induced Cellular Alterations and Senescence

Single-cell data analysis was performed on extracted human and rat skin tissues (Figure 2A), and the source of the graphical illustrations is Figdraw (www.figdraw.com). After excluding double cells, multi-cells and apoptotic cells, the final cell number was 6985–7061. In addition, the average proportion of mitochondrial genes in each cell was 0.0744–0.0789. After dimensionality reduction and clustering, these cells were divided into 11 groups. The cell types for reference are fibroblasts, T cells, smooth muscle cells, mast cells, endothelial cells, sweat gland cells, macrophage, keratinocytes, neutrophil, neural cells and NK cells (Figure 2B).

We further analyzed the cellular alterations induced by radiation, and the results showed that sweat gland cells, T cells and keratinocyte cells accounts for a relatively high proportion in normal skin. However, endothelial cells, Macrophage, mast cells, smooth muscle cells, fibroblasts and neutrophil cells accounts for a relatively high proportion in irradiated skin (Figure 2C).

We selected two well-recognized markers of senescence, CDKN1A (P21) and CDKN2A (P16), to indicate the characteristics of radiation-induced skin aging. The results showed that CDKN1A was significantly overexpressed in irradiated skin, while CDKN2A was barely detectable (Figure 2D–F). After cell annotation, we found that CDKN1A was significantly overexpressed in endothelial cells, fibroblasts, and smooth muscle cells. These cell types, which constitute a large proportion, represent the senescent cell populations in radiation-induced injury (Figure 2D).

To further illustrate the significance of CDKN1A in wound healing, we analyzed its expression changes in a normal wound healing model. The analysis results indicated that CDKN1A expression significantly increased on the first day (inflammatory phase) after acute wound formation and markedly decreased by day 7 (repair phase). The expression of CDKN1A showed no significant difference between day 7 of wound healing and the normal control group (Figure 2H). In the irradiated rat model, we found that CDKN1A remained persistently overexpressed on days 7, 14, and 28 after radiation-induced injury, highlighting the disrupted wound healing process caused by radiation (Figure 2G).

## Screening of Senescence-Related Hub Genes

The intersection of differentially expressed genes (DEGs) in radiation-damaged human skin, DEGs on day 7 in the animal model, and a list of senescence-related genes was analyzed. Ultimately, a total of 16 conserved aging-related DEGs were identified in both human and animal (Figure 3A). After filtering, a total of 13 aging-related hub genes were identified with consistent expression patterns between animals and humans. These include MMP2, IFI27, CDKN1A, IGFBP6, SPARC, VIM, IGFBP7, CTSL, CXCL14, TACSTD2, DSP, KRT15 and CLDN4 (Figure 3B).

The constructed protein-protein interaction (PPI) network revealed that CDKN1A, VIM, MMP2, IGFBP7, and CTSL occupy central positions within the interaction network (Figure 3C). In addition, pathway enrichment analysis indicated that these core genes are involved in the regulation of the cell cycle, DNA damage response, cellular senescence, senescence-associated secretory phenotype (SASP), and IGFBP-related regulation (Figure 3D).

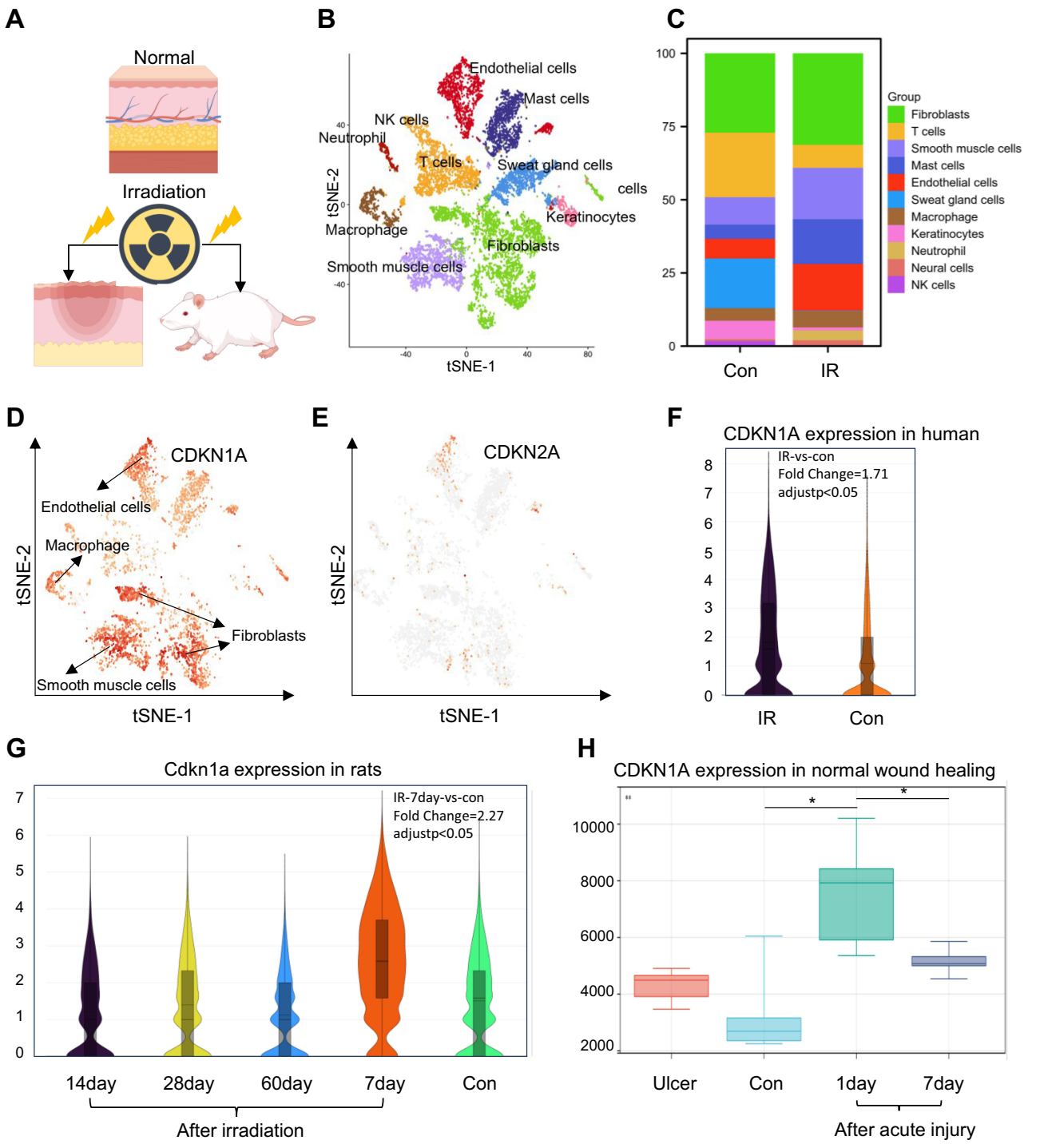


**Figure 2** Single-cell dimensionality reduction analysis and expression of senescence markers in irradiated skin. (**A**) Schematic diagram of the irradiated tissue. (**B**) Clustering of single cell populations using t-SNE. (**C**) Bar plots show the proportions that each group contributes to each cluster. (**D** and **E**) Expression of CDKN1A and CDKN2A in different cell populations. (**F** and **G**) Violin plots showing the expression levels of CDKN1A in human and rat skin. (**H**) Expression of CDKN1A and in normal wound healing and skin ulcer (venous ulcer). *P < 0.05 and **P < 0.01.

## Proteomics Analysis of BBR in the Treatment of Radiation Injury

Protein extraction was performed on cells from the control group and the BBR treatment group after irradiation (Figure 4A). The sample means were found to be at the same level, indicating good sample quality (Figure 4B). To


https://doi.org/10.2147/JIR.S523616

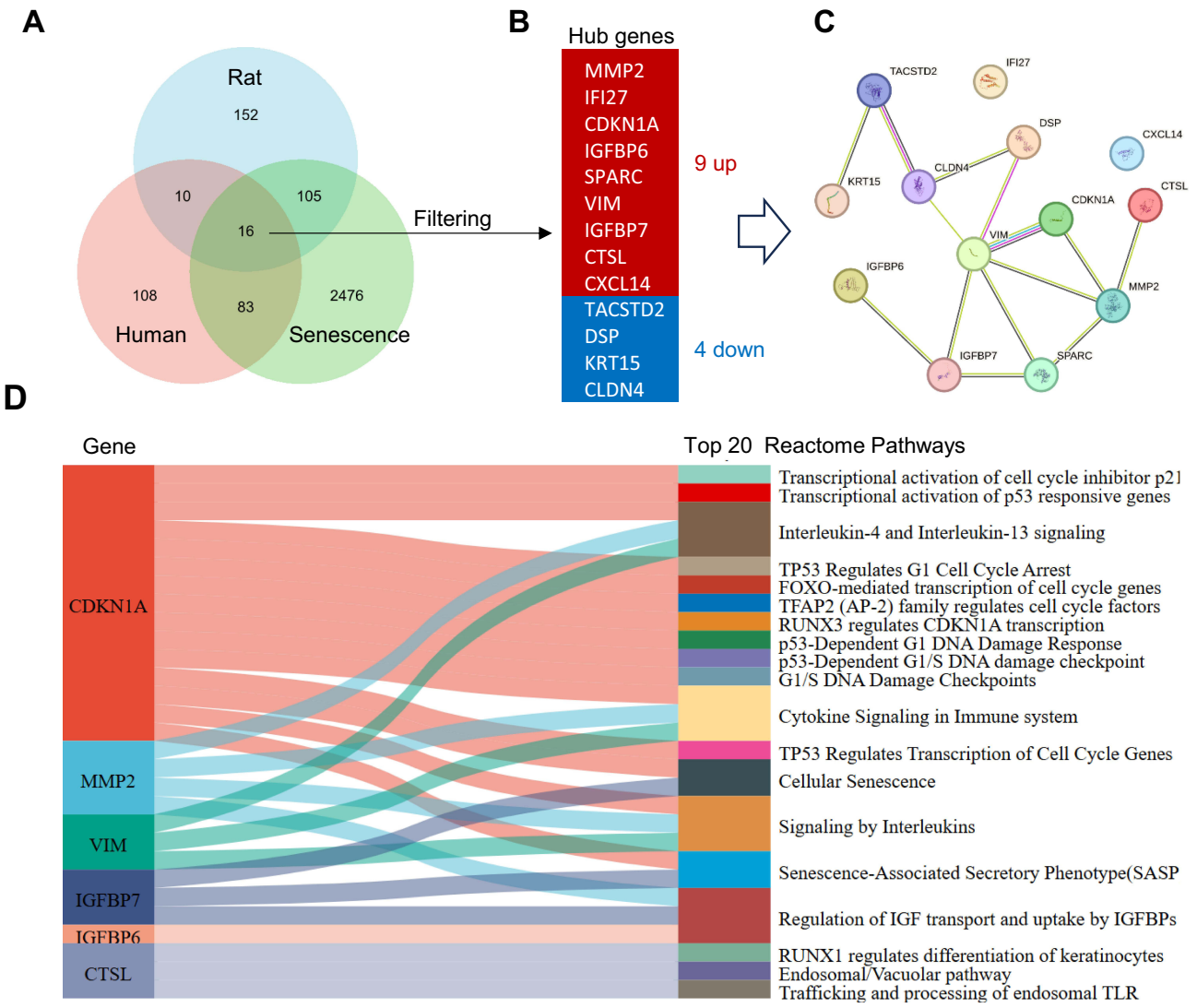


**Figure 3** Screening of senescence-related hub genes. (**A**) Venn diagram identifying common senescence-related targets in human and rat skin. (**B**) 9 commonly upregulated and 4 commonly downregulated senescence targets were identified after filtering. (**C**) Protein-protein interaction (PPI) network of senescence targets. (**D**) Pathway enrichment analysis indicated that these senescence targets are involved in the regulation of the cell cycle, DNA damage response, cellular senescence, SASP and IGFBP-related regulation.

explore the biological processes and disease mechanisms influenced by berberine (BBR) treatment, we analyzed protein expression levels under irradiation and BBR treatment conditions. The analysis revealed that BBR treatment in irradiated cells resulted in the upregulation of 199 proteins and the downregulation of 485 proteins (Figure 4C). We have provided the list of differentially expressed proteins in Supplementary File 1. BBR modulates the expression of various keratin-related proteins, such as upregulating genes like KRT14, KRT16, while downregulating genes like LRP10 and GJC1 (Figure 4D). Further subcellular localization analysis revealed that most of the differentially expressed proteins were located in the nucleus (32.31%), followed by the cytoplasm (21.35%), extracellular space (13.74%), mitochondria (13.45%), and plasma membrane (11.55%) (Figure 4E).

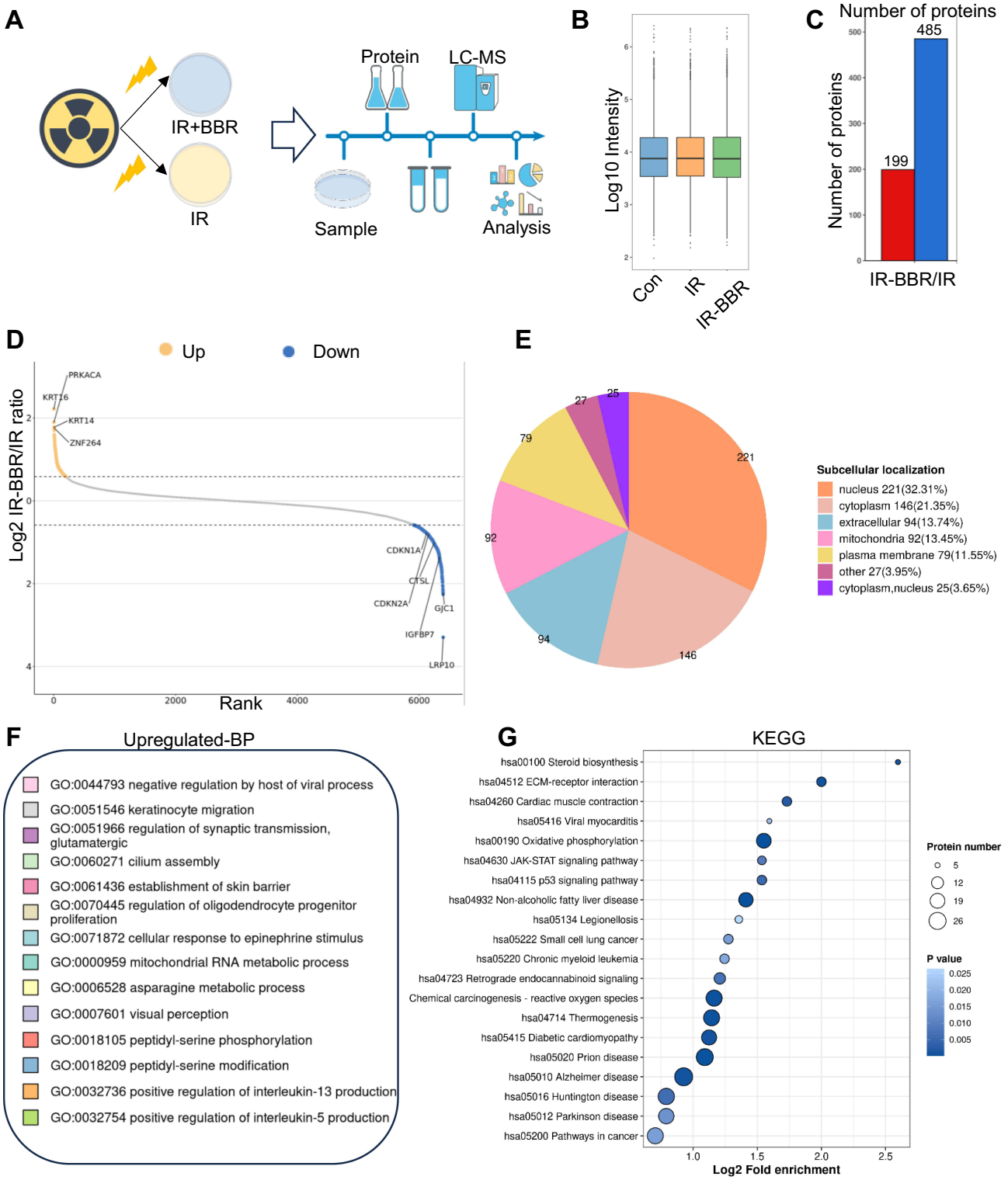


**Figure 4** Proteomics analysis of BBR in the treatment of RISI. (**A**) Schematic diagram of the protein extraction workflow. (**B**) Distribution of protein intensity values among samples. (**C**) Statistical analysis of differentially expressed proteins. (**D**) Top differential proteins with significant upregulation and downregulation. (**E**) Subcellular localization analysis of differentially expressed proteins. (**F**) Biological processes of proteins upregulated by BBR. (**G**) KEGG pathway analysis of differentially expressed proteins downregulated by BBR.


https://doi.org/10.2147/JIR.S523616

## Functional Enrichment Analysis of Differentially Expressed Proteins

GO functional analysis and KEGG pathway enrichment were performed on the 684 differentially expressed proteins, using a significance threshold of p-value < 0.05. Our analysis focused on the biological processes associated with proteins upregulated by BBR. The results revealed that BBR enhanced multiple processes, including keratinocyte migration, skin barrier establishment, and cellular response to epinephrine stimulus, among others (Figure 4F). This suggested that BBR may promote skin cell migration and facilitate the repair of radiation damage.

Given that BBR downregulated a large number of proteins (n=485), we primarily focused on pathway enrichment analysis of the signaling pathways associated with these downregulated proteins. BBR treatment downregulated several pathways related to inflammation and radiation-induced damage, including p53 signaling pathway, chemical carcinogenesis-reactive oxygen species, JAK-STAT signaling pathway and pathways in cancer (Figure 4G).

## BBR Inhibits Cellular Senescence and Regulates Senescence-Related Targets

From the proteomics analysis, three key aging-related genes (CDKN1A, IGFBP7 and CTSL) regulated by BBR were identified (Figure 5A). After BBR treatment, the expression of the senescence marker proteins CDKN1A and CDKN2A was significantly downregulated in irradiated cells (Figure 5B and C). In addition, the protein levels of IGFBP7 and CTSL were also significantly downregulated by BBR (Figure 5D and E). Single-cell analysis revealed that IGFBP7 and CTSL were significantly upregulated in radiation-induced injury and were predominantly expressed in endothelial cells, fibroblasts, and smooth muscle cells (Figure 5F–I). This expression pattern is similar to that of CDKN1A. CDKN1A is predominantly highly expressed in endothelial cells, fibroblasts, and smooth muscle cells (Figure 5J). Subsequent cellular experiments confirmed that 5Gy irradiation significantly increased the proportion of senescent cells, while treatment with 5μM BBR notably reduced the percentage of SA-β-gal-positive cells (Figure 5K and L).

## Expression Validation and Co-Expression Analysis

Further co-expression analysis revealed that IGFBP7 and CDKN1A are co-expressed in endothelial cells, fibroblasts, and smooth muscle cells, while CTSL is primarily co-expressed with CDKN1A in fibroblasts (Figure 6A and B). In irradiated rat skin, the expression of IGFBP7 and CTSL increased following irradiation, reaching its peak on the 7th day post-radiation. Subsequently, its expression levels declined on the 14th and 28th days (Figure 6C and D). We further analyzed the expression changes of these two core genes during normal wound healing. The results showed that IGFBP7 exhibited no significant changes in expression during the normal wound healing process. However, our results indicated that CTSL expression significantly increased on the first day (inflammatory phase) after acute wound formation and markedly decreased by day 7 (repair phase). In addition, CTSL was significantly upregulated in chronic ulcers (Figure 6E and F).

## Molecular Docking Results

Molecular docking aims to simulate the interaction between small-molecule ligands and large-molecule proteins, with the docking results evaluated based on binding energy (affinity). BBR exhibited good binding affinity with these core targets (Figure 7A–C). The binding energies of CDKN1A, IGFBP7 and CTSL were low, from −7.167 to −8.280 kcal·mol$^{-1}$, indicating highly stable binding (Table 1).

## BBR Promoted Cell Migration and Reduced ROS Production

The protein results showed that BBR treatment significantly increased the levels of proliferation-related protein, such as MKI67. Additionally, epithelial migration and proliferation markers, such as KRT16 and KRT17, were upregulated (Figure 8A–C). The scratch assay demonstrated that BBR enhanced cell migration ability of irradiation cells (Figure 8D and E).

Reactive oxygen species (ROS) are a key mechanism of radiation-induced damage. Proteomic analysis revealed that BBR can increase the levels of SOD2 (Figure 8F). Furthermore, BBR treatment significantly reduced intracellular ROS levels, indicating a protective effect of BBR against radiation-induced damage (Figure 8G and H).

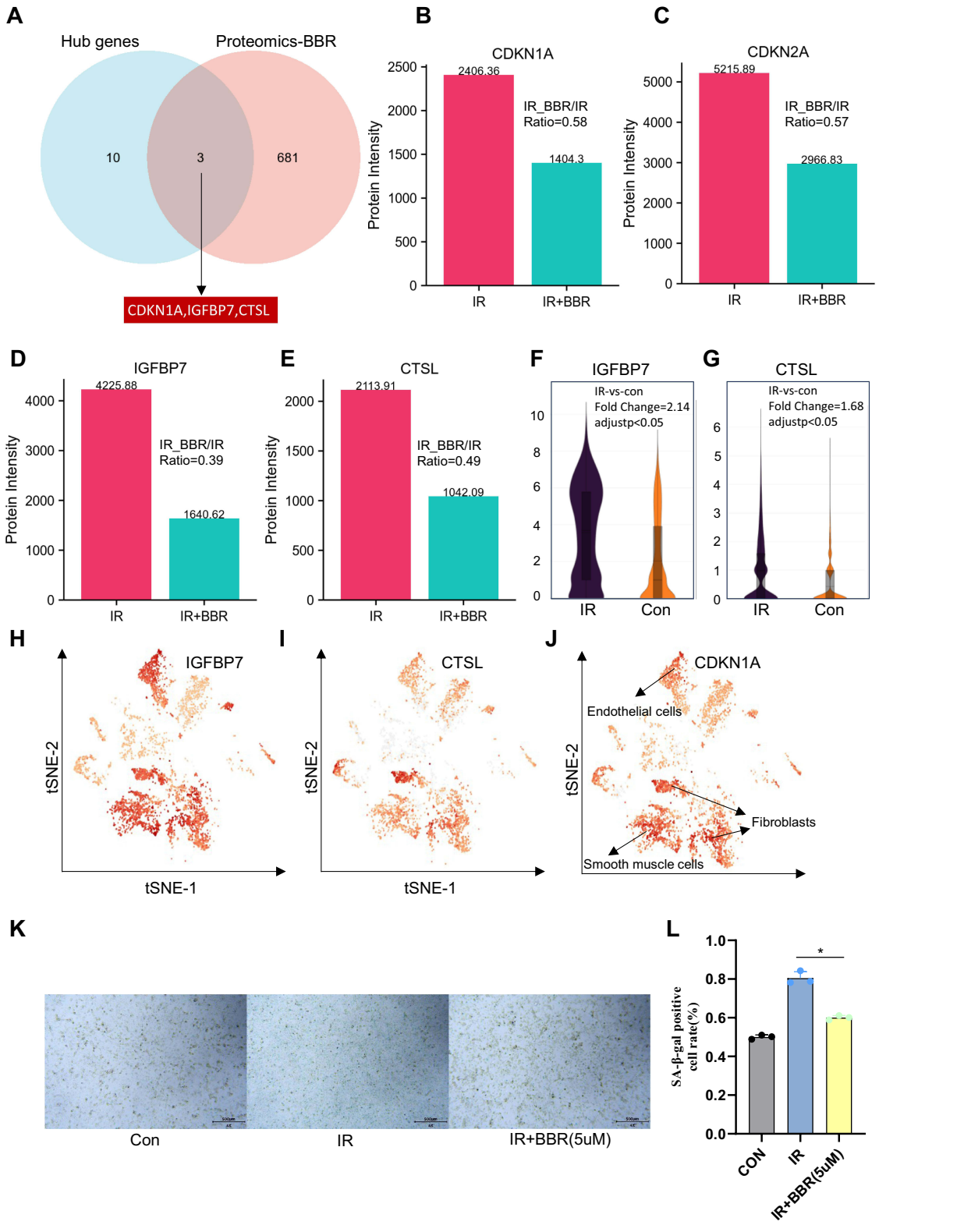


**Figure 5** BBR inhibits radiation induced cellular senescence and regulates senescence targets. (**A**) Screening of senescence targets regulated by BBR using a VENN diagram. (**B** and **C**) BBR downregulated senescence-associated protein CDKN1A and CDKN2A. (**D** and **E**) BBR downregulated senescence targets IGFBP7 and CTSL. (**F** and **G**) Violin plots showing the expression levels of IGFBP7 and CTSL in human irradiated skin. (**H–J**) Expression of IGFBP7, CTSL and CDKN1A in different cell populations. (**K** and **L**) 5 μM of BBR treatment inhibited radiation-induced endothelial cell senescence. *P < 0.05.


https://doi.org/10.2147/JIR.S523616

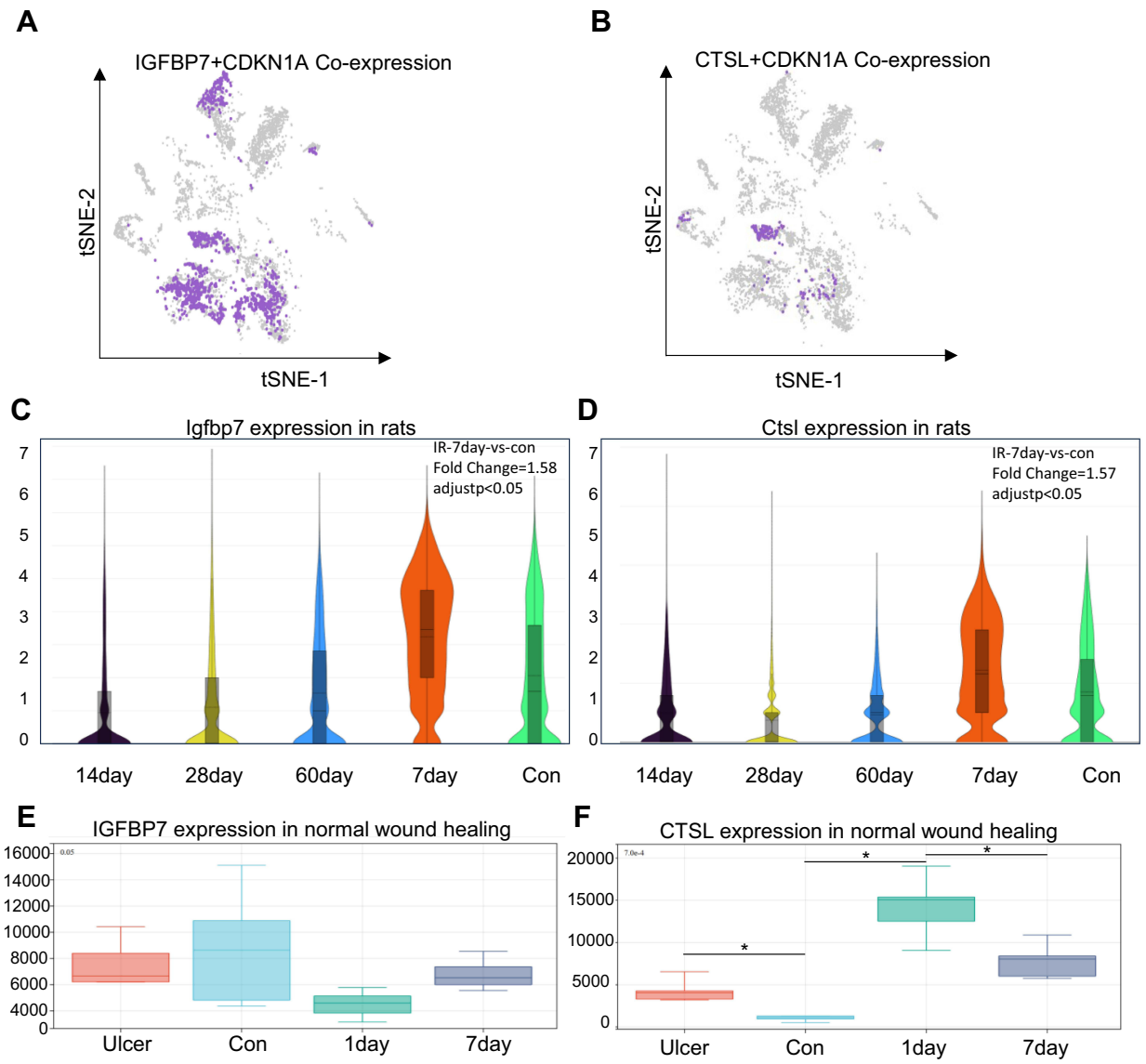


**Figure 6** Expression validation of core targets. (**A**) Co-expression analysis of IGFBP7 and CDKN1A. (**B**) Co-expression analysis of CTSL and CDKN1A. (**C** and **D**) Violin plots showing the expression levels of IGFBP7 and CTSL in rat irradiated skin. (**E** and **F**) Expression changes of IGFBP7 and CTSL in normal wound healing process and ulcer. *P < 0.05.

## BBR Regulated Senescence-Related Transcription Factors

According to the proteomic results, BBR could regulate the expression of 69 transcription factors. BBR downregulated 53 transcription factors, including several inflammation-related transcription factors such as JUND, FOSL1, and SP1 (Figure 8I). Furthermore, BBR upregulated 16 transcription factors, including longevity-associated factors such as SIRT3. Through Reactome pathway analysis, we identified six transcription factors involved in the cellular senescence pathway, including CBX6, SP1, EHMT2, UBN1, ID1, and ETS1 (Figure 8J). Finally, a regulatory network of transcription factors and aging-related targets was constructed. It was revealed that ETS1 and EHMT2 are regulators of CDKN1A, while SP1 serves as an upstream transcription factor for both CDKN1A and CTSL (Figure 8K).

## BBR Enhanced the Healing Process in Irradiated Animals

After fractionated irradiation, the body weight of irradiated animals gradually decreased, while the skin injury score progressively increased. In irradiated animals treated with BBR by gavage (Figure 9A and B), the weight loss was less

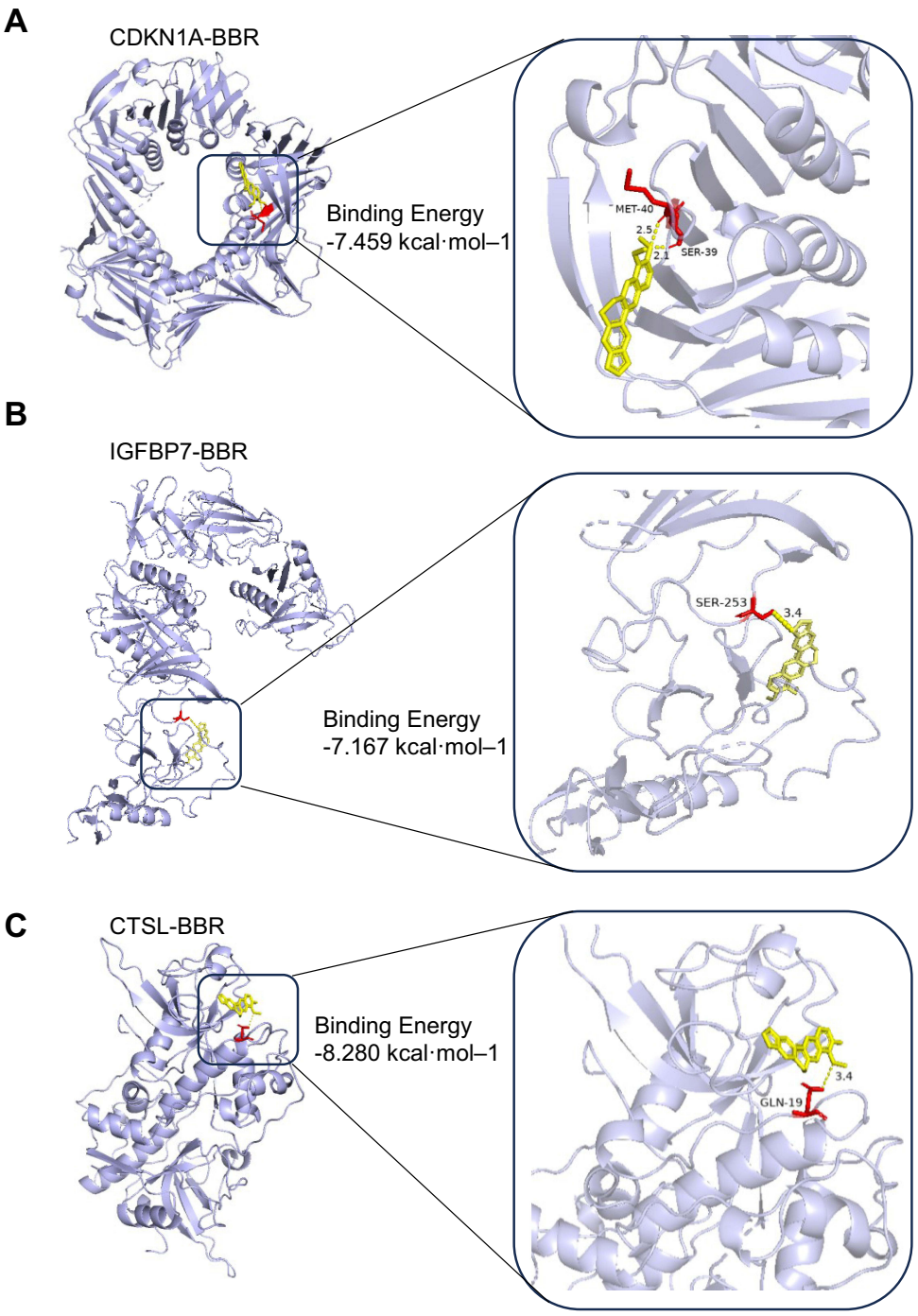


**Figure 7** Molecular docking results. (**A**–**C**) Molecular docking results of IGFBP7, CTSL and CDKN1A with BBR.

pronounced, and the skin injury score was significantly reduced compared to the standard irradiation group on the 16th day post-irradiation (Figure 9C–E). BBR significantly improved the healing process in irradiated animals. Observations revealed that animals in the irradiation-only group developed deformities and scar hyperplasia in their

**Table 1** Molecular Docking Results of BBR with Core Targets

| Protein | Ligand | Binding Energy (kcal $mol^{-1}$) | Binding Site | Applied Force |
|---|---|---|---|---|
| CDKN1A | Berberine | −7.459 | MET-40/SER-39 | Hydrogen bond |
| IGFBP7 | Berberine | −7.167 | SER-253 | Hydrogen bond |
| CTSL | Berberine | −8.280 | GLN-19 | Hydrogen bond |


https://doi.org/10.2147/JIR.S523616

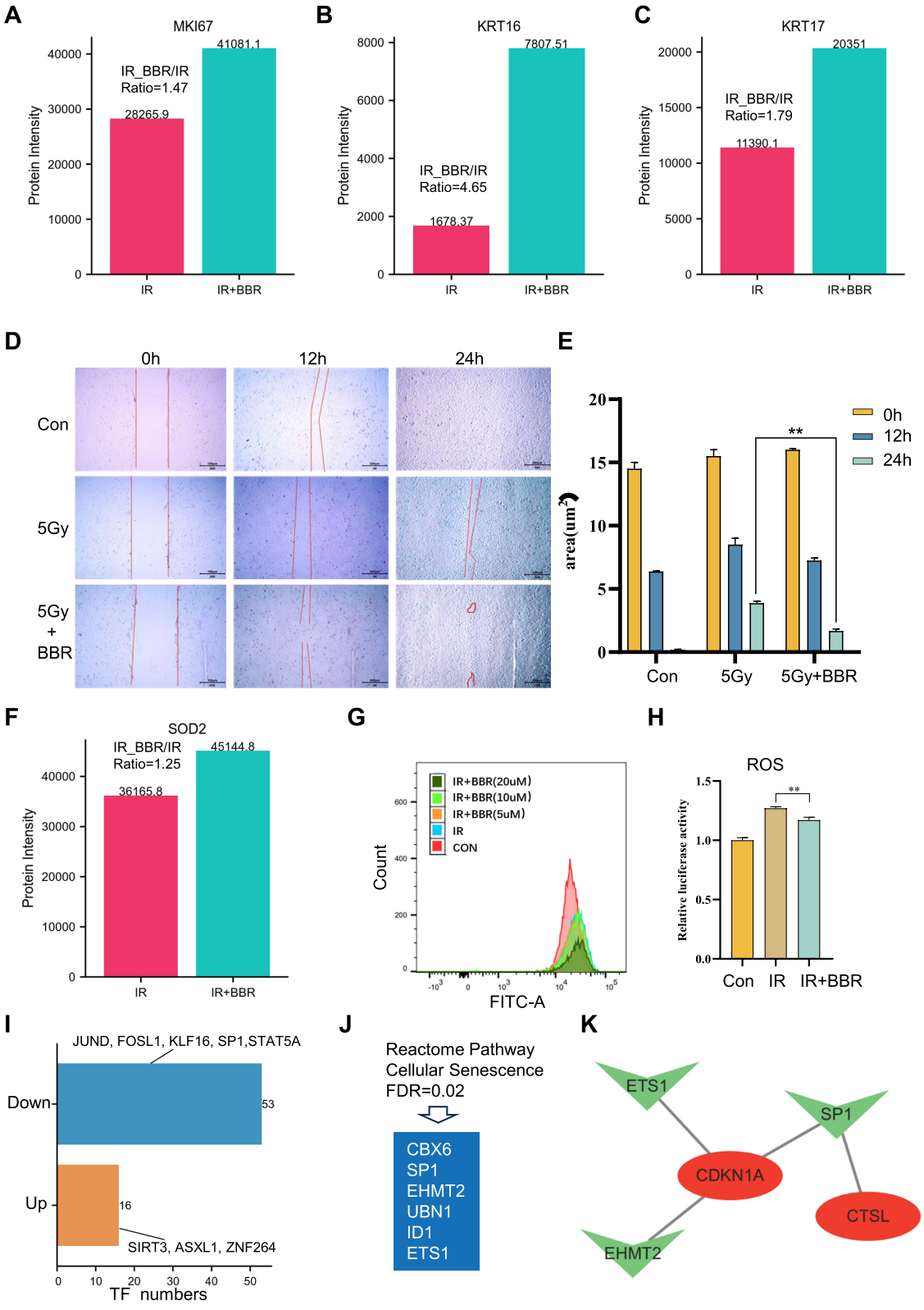


**Figure 8** BBR promoted cell migration and reduced ROS production. (**A**–**C**) BBR upregulated proliferation and epithelial migration protein MKI67, KTR16 and KRT17. (**D** and **E**) BBR promotes the migration ability of irradiated cells. (**F**) BBR upregulated antioxidant protein SOD2. (**G** and **H**) BBR reduced radiation-induced ROS generation. (**I**) BBR treatment downregulated the expression of 53 transcription factors and upregulated the expression of 16 transcription factors. (**J**) Pathway enrichment identified six transcription factors involved in the cellular senescence pathway. (**K**) The regulatory network of transcription factors and senescence targets. **P < 0.01.

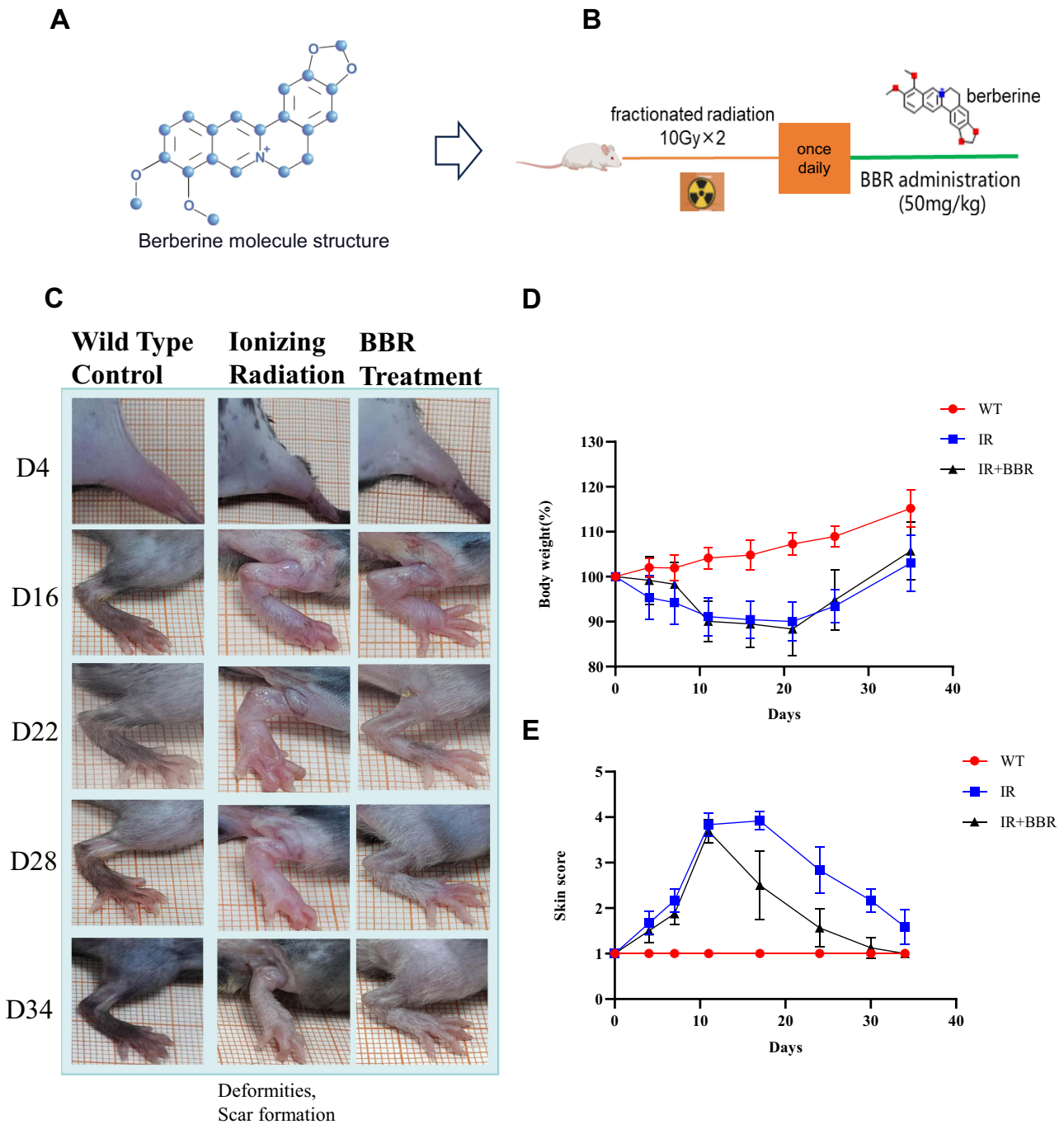


**Figure 9** BBR promotes the healing of radiation-induced skin injury in animals. (**A**) Molecular structure of BBR. (**B**) Flowchart of BBR gavage and animal irradiation procedure. (**C**) Wound healing follow-up images of animals in the control group, irradiated group, and BBR treatment group at different time points. (**D**) Changes of body weight in experimental animals after BBR treatment. (**E**) BBR treatment significantly reduced the skin injury score.

hind limbs. In contrast, mice in the BBR-treated group exhibited normal skin and hair growth, with no significant local deformities or scar hyperplasia observed (Figure 9C).

## Discussion

Radiation-induced skin injury (RISI) remains a significant clinical challenge due to its multifaceted pathophysiology, involving oxidative stress, DNA damage, and inflammation.[22] Thus far, the underlying mechanisms and regulatory networks of radiation injury remain unclear. This study utilized single-cell sequencing of radiation-induced skin injury


https://doi.org/10.2147/JIR.S523616

samples to uncover the molecular and cellular changes associated with radiation damage. In addition, we propose Berberine (BBR), a traditional Chinese medicine, as a potential treatment for radiation-induced injury. This study investigated the effects of BBR on RISI, focusing on its role in modulating senescence, inflammation, and wound healing mechanisms. The findings provide new insights into the mechanisms of RISI and potential therapeutic benefits of BBR for managing radiation damage.

The transcriptomic analysis of irradiated skin revealed a distinct pattern of gene expression changes, with 217 differentially expressed genes (DEGs) identified. Upregulated genes such as S100A8 and S100A9 underscore the inflammatory response elicited by radiation exposure,[35] whereas downregulated genes, including AQP5 and KRT15, highlight the disruption of skin barrier integrity.[37,38] Functional enrichment analysis further implicated pathways associated with immune response, cellular senescence, and tumor-related signaling, such as the TNF, p53, and NF-kappa B pathways, as critical drivers of radiation-induced damage.[39,40]

The upregulation of senescence markers, particularly CDKN1A,[41] in endothelial cells, fibroblasts, and smooth muscle cells, supports the role of cellular senescence as a central feature of RISI. Persistent overexpression of CDKN1A during the repair phase, as observed in both human and animal models, correlates with impaired wound healing, contrasting with the transient expression observed in normal acute wound healing. These findings align with the concept that sustained senescence disrupts the repair processes, contributing to chronic skin injury.[42,43]

Berberine treatment demonstrated a capacity to modulate the deleterious effects of radiation. Proteomic analysis identified a significant downregulation of inflammation and damage associated pathways, including p53 signaling and ROS related carcinogenesis.[44] Simultaneously, BBR enhanced pathways involved in skin repair, such as keratinocyte migration and the establishment of the skin barrier.[45] Notably, BBR effectively reduced the expression of key senescence markers, including CDKN1A, IGFBP7, and CTSL, while promoting the expression of repair-associated proteins like KRT16 and MKI67.[46,47] These results suggest that BBR mitigates senescence-associated dysfunction and promotes epithelial proliferation and migration.

The molecular docking results indicate stable binding interactions between BBR and core senescence-related proteins, such as CDKN1A, IGFBP7, and CTSL, providing a mechanistic basis for its modulatory effects. These interactions may underlie BBR's ability to downregulate senescence markers and alleviate the senescence-associated secretory phenotype (SASP), which exacerbates inflammation and tissue damage.[47] Our results suggest that IGFBP7 may serve as a key component of SASP in radiation-induced skin injury.[48] This is evidenced by its co-expression with the senescence marker CDKN1A in senescent cells following radiation exposure, whereas its expression remains unchanged in normal wound healing processes. Our study further constructed a transcription factor regulatory network associated with senescence genes, identifying SP1 as a potential upstream mediator through which Berberine (BBR) inhibits radiation-induced skin aging.[49]

In vivo experiments further confirmed the therapeutic potential of BBR. Animals treated with BBR exhibited reduced skin injury scores, improved body weight retention, and enhanced wound healing compared to untreated irradiated controls. These observations are consistent with the in vitro findings and underscore the translational potential of BBR as a therapeutic agent for RISI. It should be noted that our study used male mice to exclude the influence of estrogen on wound healing.

While these findings are promising, there are limitations to this study. The exact molecular pathways through which BBR exerts its effects on senescence and wound repair require further elucidation. In subsequent studies, further research is still needed to investigate the effects of BBR on radiation damage in female animals. This study primarily demonstrated that BBR treatment promoted skin wound healing in irradiated animals. However, radiation-induced damage also includes long-term complications such as recurrence and skin fibrosis. Although none of the BBR-treated animals in this study exhibited recurrent skin lesions, future research should further investigate the drug's effects on skin fibrosis, as well as vascular and neural regeneration. Additionally, the long-term safety and efficacy of BBR in clinical settings remain to be validated. Future studies should explore the combined use of BBR with other therapeutic modalities to achieve synergistic effects and improve patient outcomes.

In conclusion, this study reveals that radiation damage leads to excessive inflammation in skin tissues and cellular senescence in skin cells. Our results highlight the protective effects of BBR against radiation-induced skin injury,

mediated through its anti-senescence, anti-inflammatory, and wound-healing properties. By targeting critical senescence markers such as CDKN1A, IGFBP7, and CTSL, as well as pivotal signaling pathways like p53, ROS, and JAK-STAT, BBR presents itself as a potential therapeutic agent for managing RISI. This approach aims to address both the clinical manifestations and the fundamental pathophysiological mechanisms associated with this condition.

## Availability of Supporting Data

All data discussed in this publication have been deposited in NCBI's Gene Expression Omnibus[50] and are accessible through GEO Series accession number GSE193564, GSE193807 and GSE174661.

## Ethics Approval and Consent to Participate

This study was approved by the Medical Ethics Committee of the second affiliated hospital of Chengdu Medical College. All participants provided written informed consent.

## Author Contributions

All authors made a significant contribution to the work reported, whether that is in the conception, study design, execution, acquisition of data, analysis and interpretation, or in all these areas; took part in drafting, revising or critically reviewing the article; gave final approval of the version to be published; have agreed on the journal to which the article has been submitted; and agree to be accountable for all aspects of the work.

## Funding

This work was supported by the China National Nuclear Corporation's 2021 "Nuclear Medicine Technology Innovation" Project (ZHYLZD2023004, ZHYLYB2021009). Natural Science Project of Chengdu Medical College and the Second Affiliated Hospital Joint Fund Project (CYZYB23-02, 2022LHFSZYB-08). Sichuan Province Science and Technology Innovation Project (Seedling Project, MZGC20240019). Sichuan Medical Association Wound Disease (Taige) Special Research Project (2023TG14).

## Disclosure

Authors in this study do not have any Competing-Interest.

## References

1. Deng G, Li J, Li Y, et al. Evolution of radiation-induced dermatitis treatment. *Clin Transl Oncol*. 2024;26(9):1968–1975. doi:10.1007/s12094-024-03418-3
2. Amanda R, Rachel I, Ronald M. Management of acute radiation dermatitis: a review of the literature and proposal for treatment algorithm. *J Am Acad Dermatol*. 2019;81(2):558–567.
3. Yang X, Ren H, Guo X, Hu C, Fu J. Radiation-induced skin injury: pathogenesis, treatment, and management. *Aging*. 2020;12(22):23379.
4. Matsuda K, Kurohama H, Kuwatsuka Y, Iwanaga A, Murota H, Nakashima M. Detection of genome instability by 53BP1 expression as a long-lasting health effect in human epidermis surrounding radiation-induced skin cancers. *J Radiat Res*. 2024;65:i57–66.
5. Chen Y, Ma L, Cheng Z, et al. Senescent fibroblast facilitates re-epithelization and collagen deposition in radiation-induced skin injury through IL-33-mediated macrophage polarization. *J Transl Med*. 2024;22(1):176.
6. Cui J, Wang TJ, Zhang YX, et al. Molecular biological mechanisms of radiotherapy-induced skin injury occurrence and treatment. *Biomed Pharmacother*. 2024;180:117470.
7. Saurabh S, Prajwal G. A comprehensive review of sensors of radiation-induced damage, radiation-induced proximal events, and cell death. *Immunol Rev*. 2024.
8. Abe JI, Allen BG, Beyer AM, et al. Radiation-induced macrovessel/microvessel disease. *Arterioscler Thromb Vasc Biol*. 2024;44(12):2407–2415.
9. Tamarat R, Satyamitra MM, Benderitter M, DiCarlo AL. Radiation-induced gastrointestinal and cutaneous injuries: understanding models, pathologies, assessments, and clinically accepted practices. *Int J Radiat Biol*. 2024;100(7):969–981.
10. Yang P, Zhang S, Yan T, Li F, Zhang S. The therapeutic application of stem cells and their derived exosomes in the treatment of radiation-induced skin injury. *Radiat Res*. 2023;199(2):182–201.
11. Wang YY, Yu DJ, Zhao TL, et al. Successful rescue of the victim exposed to a super high dose of iridium-192 during the Nanjing radiological accident in 2014. *Radiat Res*. 2019;191(6):527–531.
12. Sun A, Yang H, Li T, et al. Molecular mechanisms, targets and clinical potential of berberine in regulating metabolism: a review focussing on databases and molecular docking studies. *Front Pharmacol*. 2024;15:1368950.
13. Okoye GA, Bui H, Zadu A, Myles IA, Byrd AS. The multifaceted effects of berberine: potential uses in dermatology. *J Drugs Dermatol*. 2025;24(3):298–301.

14. Zhu Y, Tian Q, Huang Q, Wang J. Bile-processed rhizoma coptidis alleviates type 2 diabetes mellitus through modulating the gut microbiota and short-chain fatty acid metabolism. *Int Immunopharmacol*. 2025;156:114645.
15. Tan HL, Chan KG, Pusparajah P, et al. Rhizoma Coptidis: a Potential Cardiovascular Protective Agent. *Front Pharmacol*. 2016;7:362.
16. Liu Y, Yu H, Zhang C, et al. Protective effects of berberine on radiation-induced lung injury via intercellular adhesion molecular-1 and transforming growth factor-beta-1 in patients with lung cancer. *Eur J Cancer*. 2008;44(16):2425–2432.
17. Li G, Zhang Y-P, Tang J-L, et al. Effects of berberine against radiation-induced intestinal injury in mice. *Int J Radiat Oncol Biol Phys*. 2010;77 (5):1536–1544. doi:10.1016/j.ijrobp.2010.02.062
18. Jiang C, Lao G, Ran J, et al. Berberine alleviates AGEs-induced ferroptosis by activating NRF2 in the skin of diabetic mice. *Exp Biol Med*. 2024;249:10280.
19. Kulkarni SK, Dandiya PC, Varandani NL. Pharmacological investigations of berberine sulphate. *Jpn J Pharmacol*. 1972;22(1):11–16. doi:10.1016/S0021-5198(19)31702-0
20. Song J, Zhang H, Wang Z, et al. The role of FABP5 in radiation-induced human skin fibrosis. *Radiat Res*. 2017;189(2):177–186.
21. Butler A, Hoffman P, Smibert P, Papalexi E, Satija R. Integrating single-cell transcriptomic data across different conditions, technologies, and species. *Nat Biotechnol*. 2018;36(5):411–420.
22. Yan T, Yang P, Bai H, et al. Single-cell RNA-Seq analysis of molecular changes during radiation-induced skin injury: the involvement of Nur77. *Theranostics*. 2024;14(15):5809.
23. Hao Y, Stuart T, Kowalski MH, et al. Dictionary learning for integrative, multimodal and scalable single-cell analysis. *Nat Biotechnol*. 2023;42 (2):293–304.
24. Aran D, Looney AP, Liu L, et al. Reference-based analysis of lung single-cell sequencing reveals a transitional profibrotic macrophage. *Nat Immunol*. 2019;20(2):163–172.
25. Mabbott NA, Baillie J, Brown H, et al. An expression atlas of human primary cells: inference of gene function from coexpression networks. *BMC Genomics*. 2013;14(1):632. doi:10.1186/1471-2164-14-632
26. Stelzer G, Rosen N, Plaschkes I, et al. The GeneCards suite: from gene data mining to disease genome sequence analyses. *Curr Protoc Bioinformatics*. 2016;54:1–30.
27. Liu Z, Zhang L, Toma MA, et al. Integrative small and long RNA omics analysis of human healing and nonhealing wounds discovers cooperating microRNAs as therapeutic targets. *Elife*. 2022;11:e80322.
28. Milacic M, Beavers D, Conley P, et al. The reactome pathway knowledgebase 2024. *Nucleic Acids Res*. 2023;52:D672–8.
29. Xu W, Velankar S, Patwardhan A, et al. Announcing the launch of protein data bank china as an associate member of the worldwide protein data bank partnership. *Acta Crystallogr D Struct Biol*. 2023;79:792–795.
30. Forli S, Huey R, Pique ME, et al. Computational protein-ligand docking and virtual drug screening with the AutoDock suite. *Nat Protoc*. 2016;11 (5):905–919.
31. Liu Y, Sun L, Li Y, Holmes C. Mesenchymal stromal/stem cell tissue source and in vitro expansion impact extracellular vesicle protein and miRNA compositions as well as angiogenic and immunomodulatory capacities. *J Extracell Vesicles*. 2024;13(8):e12472.
32. Tu W, Tang S, Yan T, et al. Integrative multi-omic analysis of radiation-induced skin injury reveals the alteration of fatty acid metabolism in early response of ionizing radiation. *J Dermatol Sci*. 2023;108(3):178–186.
33. Kumar S, Kolozsvary A, Kohl R, Lu M, Brown S, Kim JH. Radiation-induced skin injury in the animal model of scleroderma: implications for post-radiotherapy fibrosis. *Radiat Oncol*. 2008;3:40.
34. Geng F, Zhong L, Yang T, et al. A frog skin-derived peptide targeting SCD1 exerts radioprotective effects against skin injury by inhibiting STING-mediated inflammation. *Adv Sci*. 2024;11(25):2306253.
35. Franz S, Torregrossa M, Anderegg U, et al. Dysregulated S100A9 expression impairs matrix deposition in chronic wounds. *Int J Mol Sci*. 2024;25 (18):9980. doi:10.3390/ijms25189980
36. Meng Q, Ning J, Lu J, et al. Cmtm4 deficiency exacerbates colitis by inducing gut dysbiosis and S100a8/9 expression. *J Genetics Genomics*. 2024;51(8):811–823. doi:10.1016/j.jgg.2024.03.009
37. Fu L, Zhao Z, Zhao S, et al. The involvement of aquaporin 5 in the inflammatory response of primary Sjogren's syndrome dry eye: potential therapeutic targets exploration. *Front Med*. 2024;11:1439888. doi:10.3389/fmed.2024.1439888
38. Li Y, Dong L, Chen Y, et al. Epithelial differentiation of gingival mesenchymal stem cells enhances re-epithelialization for full-thickness cutaneous wound healing. *Stem Cell Res Ther*. 2024;15(1):455. doi:10.1186/s13287-024-04081-9
39. Zhang M, Kang N, Yu X, et al. Author Correction: TNF inhibitors target a mevalonate metabolite/TRPM2/calcium signaling axis in neutrophils to dampen vasculitis in Behçet's disease. *Nat Commun*. 2025;16(1):366. doi:10.1038/s41467-024-55702-z
40. Liang J, Chen M, Yan G, et al. Donafenib activates the p53 signaling pathway in hepatocellular carcinoma, induces ferroptosis, and enhances cell apoptosis. *Clin Exp Med*. 2025;25(1):29. doi:10.1007/s10238-024-01550-6
41. Yu G, Ganier C, Allison DB, et al. Mapping epidermal and dermal cellular senescence in human skin aging. *Aging Cell*. 2024;24(1):e14358. doi:10.1111/acel.14358
42. Yu G, Gomez PT, Prata LG, et al. Clinicopathological and cellular senescence biomarkers in chronic stalled wounds. *Int J Dermatol*. 2024;63 (9):1227–1235. doi:10.1111/ijd.17072
43. Yu G, Monie DD, Khosla S, et al. Mapping cellular senescence networks in human diabetic foot ulcers. *GeroScience*. 2024;46(1):1071–1082. doi:10.1007/s11357-023-00854-x
44. Sun Q, Ye Z, Qin Y, et al. Oncogenic function of TRIM2 in pancreatic cancer by activating ROS-related NRF2/ITGB7/FAK axis. *Oncogene*. 2020;39(42):6572–6588. doi:10.1038/s41388-020-01452-3
45. Liu Z, Bian X, Luo L, et al. Spatiotemporal single-cell roadmap of human skin wound healing. *Cell Stem Cell*. 2024;32(3):479–498.
46. Zhang X, Yin M, Zhang L. Keratin 6, 16 and 17-critical barrier alarmin molecules in skin wounds and psoriasis. *Cells*. 2019;8(8):807. doi:10.3390/cells8080807
47. Zhang K, Xu R, Zheng L, et al. Elevated N-glycosylated cathepsin L impairs oocyte function and contributes to oocyte senescence during reproductive aging. *Aging Cell*. 2024;24(2):e14397. doi:10.1111/acel.14397
48. Tong Z, Wu J, Gong Q, Yuan Y, Wang S, Jiang W. Insulin-like growth factor binding protein 7 identified in aged dental pulp by single-cell RNA sequencing. *J Adv Res*. 2024.

49. Ying Z, Zhai H, Zhang S, et al. Sonic hedgehog restrains the ubiquitin-dependent degradation of SP1 to inhibit neuronal/glial senescence associated phenotypes in chemotherapy-induced peripheral neuropathy via the TRIM25-CXCL13 axis. *J Adv Res*. 2024;73:501–515. doi:10.1016/j.jare.2024.08.001
50. Edgar R, Domrachev M, Lash AE. Gene expression omnibus: NCBI gene expression and hybridization array data repository. *Nucleic Acids Res*. 2002;30(1):207–210. doi:10.1093/nar/30.1.207